Accepted Manuscript

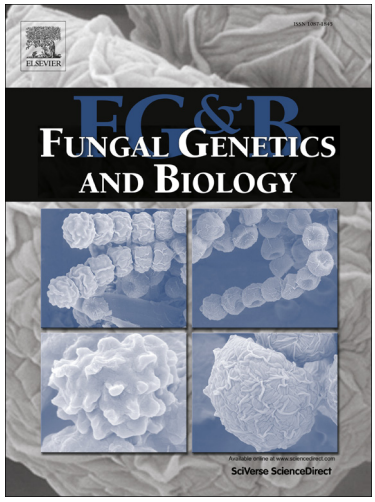

A cerato-platanin-like protein HaCPL2 from *Heterobasidion annosum sensu stricto* induces cell death in *Nicotiana tabacum* and *Pinus sylvestris*

Hongxin Chen, Julia Quintana, Andriy Kovalchuk, Wimal Ubhayasekera, Fred O. Asiegbu

PII: S1087-1845(15)30031-1
DOI: http://dx.doi.org/10.1016/j.fgb.2015.09.007
Reference: YFGBI 2898

To appear in: *Fungal Genetics and Biology*

Received Date: 23 April 2015
Revised Date: 11 September 2015
Accepted Date: 14 September 2015

Please cite this article as: Chen, H., Quintana, J., Kovalchuk, A., Ubhayasekera, W., Asiegbu, F.O., A cerato-platanin-like protein HaCPL2 from *Heterobasidion annosum sensu stricto* induces cell death in *Nicotiana tabacum* and *Pinus sylvestris*, *Fungal Genetics and Biology* (2015), doi: http://dx.doi.org/10.1016/j.fgb.2015.09.007

A cerato-platanin-like protein HaCPL2 from *Heterobasidion annosum sensu stricto* induces cell death in *Nicotiana tabacum* and *Pinus sylvestris*.

Hongxin Chen[1]*, Julia Quintana[1], Andriy Kovalchuk[1], Wimal Ubhayasekera[2], Fred O. Asiegbu[1]

[1]Department of Forest Sciences, P.O. Box 27, Latokartanonkaari 7, 00014, University of Helsinki, Helsinki, Finland; [2]Department of Cell and Molecular Biology, Uppsala University, Box 596, Biomedical Center, SE-751 24, Uppsala, Sweden.

* Author for correspondence: Department of Forest Sciences, P.O. Box 27, Latokartanonkaari 7, 00014, University of Helsinki, Helsinki, Finland. Tel: +358 453400485. E-mail: hongxin.chen@helsinki.fi

Abstract

The cerato-platanin family is a group of small secreted cysteine-rich proteins exclusively from filamentous fungi. They have been shown to be involved in the interactions between fungi and plants. Functional characterization of members from this family has been performed mainly in Ascomycota, except *Moniliophthora perniciosa*. Our previous phylogenetic analysis revealed that recent gene duplication of cerato-platanins has occurred in Basidiomycota but not in Ascomycota, suggesting higher functional diversification of this protein family in Basidiomycota than in Ascomycota. In this study, we identified three cerato-platanin homologues from the basidiomycete conifer pathogen *Heterobasidion annosum sensu stricto*. Expression of the homologues under various conditions as well as their roles in the *H. annosum s.s.-Pinus sylvestris* (Scots pine) pathosystem was investigated. Results showed that HaCPL2 (cerato-platanin-like protein 2) had the highest sequence similarity to cerato-platanin from *Ceratocystis platani* and *hacpl2* was significantly induced during nutrient starvation and necrotrophic growth. The treatment with recombinant HaCPL2 induced cell death, phytoalexin production and defense gene expression in *Nicotiana tabacum*. Eliciting and cell death-inducing ability accompanied by retardation of apical root growth was also demonstrated in Scots pine seedlings. Our results suggest that HaCPL2 might contribute to the virulence of *H. annosum s.s.* by promoting plant cell death.

Keywords: fungal elicitor, fungal effector, phytotoxicity, pathogenesis, plant defense

1. Introduction

Heterobasidion annosum sensu lato is a basidiomycete species complex comprising five species that are widely distributed in Europe, North America, China, Japan and parts of Russia. In these regions, they cause great economical losses every year (Dai and Korhonen, 1999; Dai et al., 2003). One of the species in the complex, *Heterobasidion annosum sensu stricto*, is a major causal agent of root and butt rot disease of conifers in the Northern Hemisphere (Asiegbu et al., 2005). It can live as a saprotroph or a necrotroph and switch the life style depending on substrate availability. The fungus produces both basidiospores and conidiospores, but primary infection is mostly mediated by the former through freshly exposed wood surfaces, such as stumps tops or stem and root wounds, and may spread through root contacts or grafts (Garbelotto and Gonthier, 2013). As a necrotrophic fungus, it secretes some cell-wall-degrading enzymes and toxins (fommanoxin, fommanosin, fommanoxin acid, oosponol and oospoglycol), which can modify host cell functions. Many of these molecules might contribute to the virulence of the pathogen (Asiegbu et al., 2005). The current knowledge about the function of specific effectors or necrosis-inducing molecules in this conifer pathogen is still very limited.

Our previous transcriptomic study, where over 12,000 *H. annosum s.s.* genes were analysed, uncovered cerato-platanins as stress-responsive genes during abiotic (Raffaello et al., 2014) and biotic stimuli (Jaber et al., unpublished). This is a group of small secreted cysteine-rich proteins that are specific for filamentous fungi. They are located in the fungal cell wall (Boddi et al., 2004) and secreted extracellularly (Pazzagli et al., 2014). Many cerato-platanins have been identified as major secreted proteins from culture filtrates (Hall et al., 1999; Pazzagli et al., 1999; Djonovic et al., 2006; Seidl et al., 2006; Frias et al., 2011). This could indicate their potential roles in general fungal development and fungus-host interactions. Indeed, cerato-platanin expression is down-regulated in the condition where fungal growth is reduced and up-regulated during chlamydospore formation (Baccelli et

al., 2012). On the other hand, cerato-platanins have been found to act as fungal elicitors or phytotoxins in host and non-host plants (Pazzagli et al., 2014). For example, elicitor Sm1 from *Trichoderma virens* is able to induce plant defense responses, such as defense-related gene expression and production of reactive oxygen species, and required for systemic resistance against pathogens (Djonovic et al., 2006; Djonovic et al., 2007). Likewise, some cerato-platanins from plant pathogens, such as cerato-platanin from *Ceratocystis platani*, BcSpl1 from *Botrytis cinerea* and MpCP1 from *Moniliophthora perniciosa*, are induced during infection and able to cause necrosis and hypersensitive response (HR) (Pazzagli et al., 1999; Frias et al., 2011; de O. Barsottini et al., 2013). 3D structures of several cerato-platanins show high similarity to expansins, endoglucanases and barwins from plants, which helps to explain the eliciting and necrosis-inducing ability (de Oliveira et al., 2011; de O. Barsottini et al., 2013; Pazzagli et al., 2014). Indeed, cerato-platanin from *C. platani* is able to bind *N*-acetylglucosamine oligomers, chitin and colloidal chitin and loosen cellulosic materials via a non-enzymatic mechanism (de Oliveira et al., 2011; Baccelli et al., 2014b). All of these activities are similar to those described for expansins (Pazzagli et al., 2014).

Although several efforts have been made towards a deeper understanding of the pathogenesis mechanism of *H. annosum s.s.*, very little is known about proteins that contribute to the virulence of the pathogen. Meanwhile, almost all functional studies of cerato-platanins were carried out in ascomycetes, except *M. perniciosa*, the basidiomycete causal agent of witches' broom disease in *Theobroma cacao*. This makes cerato-platanins potentially good candidates to gain insight the determinants of the virulence in the *H. annosum s.s.-Pinus sylvestris* (Scots pine) pathosystem and at the same time contributes to the knowledge of cerato-platanins from basidiomycetes. In this study, we were able to demonstrate the eliciting and cell death-inducing ability of HaCPL2 (cerato-platanin-like protein 2) from *H. annosum s.s.* on host and non-host plants.

2. Materials and methods

2.1 Fungal and plant materials

H. annosum s.s. P-type (isolate 03012) was kindly provided by Kari Korhonen (LUKE, Finland) and maintained on solid MEA medium (2% malt extract and 1.5% agar) at 20°C. The Scots pine seeds (*P. sylvestris* L., Saleby FP-45) were purchased from SVEASKOG (Sweden). Prior to use, seeds were sterilized by soaking in 33% H_2O_2 for 15 min, rinsed 5 times with sterilized water and sown on 1% water agar plates. Plates were kept in controlled conditions in a growth chamber (12-h light/12-h dark photoperiod with 80% relative humidity at 24°C). Seeds of *Nicotiana tabacum* cv.SR1 were germinated and grown in soil/vermiculite mixture (3:1) in a plant growth room under controlled conditions (16-h light/8-h dark period with 80% relative humidity at 22°C).

2.2 Gene cloning and sequence analysis

Cerato-platanin homologue sequences were obtained by PCR using the Phusion DNA polymerase (Thermo Scientific). Genomic DNA and cDNA derived from two-week-old mycelia grown on solid MEA media were used as the templates, respectively. The gene-specific primers for full-length *hacpl1*, *hacpl2* and *hacpl3* were designed based on the cerato-platanin homolog sequences from a closely related species *Heterobasidion irregulare* (transcript IDs: 41461, 146085 and 145203 in *H. irregulare* assembly v2.0 available from MycoCosm database at Joint Genome Institute (http://genome.jgi-psf.org/Hetan2/Hetan2.home.html)). Primers used for cloning are listed in Supplementary Table 1. The PCR program for all three homologues was as follow: 98°C 3 min, 30 cycles (98°C 30 s, 61°C 30 s and 72°C 1 min), 72°C 10 min, 4°C hold. PCR products were separated in 1% agarose gel, purified by the GenElute™ Gel Extraction Kit (Sigma-Aldrich), cloned into pGEM®-T Easy vector (Promega) and transformed into TOP10F´ *E. coli* cells (Invitrogen) according to the

manufacturers' instructions. Positive transformants were confirmed by colony PCR and *EcoR I* restriction enzyme digestion (Thermo Scientific) and sent for sequencing (Haartman Institute, Finland). Sequences were submitted to SignalP 4.1 Server (http://www.cbs.dtu.dk/services/SignalP/) for signal peptide prediction and InterProScan (http://www.ebi.ac.uk/interpro/search/sequence-search) for conserved domain prediction. Sequences were also aligned and compared with the reference protein cerato-platanin from *C. platani* (GenBank accession number: CAC84090.2) with MUSCLE (default settings) in JALVIEW (Waterhouse et al., 2009).

2.3 Growth under abiotic stress

For abiotic stress, effects of osmotic ($NaCl/CaCl_2$), oxidative (H_2O_2) and starvation conditions on gene expression were tested. Three biological replicates were carried out for each treatment. As a control, *H. annosum s.s.* was grown in liquid MEG medium (0.5% malt extract and 0.5% glucose) at 20°C for two weeks. For osmotic and oxidative stress, the fungus was grown initially in MEG at 20°C for two weeks followed by exposure to 0.5 M NaCl, 0.5 M $CaCl_2$ or 5 mM H_2O_2 for 1 hour, respectively. For nutrient starvation, the fungus was first grown in MEG at 20°C for two weeks. Mycelia were then washed three times with autoclaved Milli-Q water, placed in 100 ml autoclaved Milli-Q water with 100 µl 0.2 g/ml glucose solution and incubated at 20°C for 5 days. Samples were then harvested and frozen in liquid nitrogen followed by RNA extraction according to the previous study (Raffaello et al., 2012).

2.4 Growth during different nutrition modes

Cerato-platanin-like gene expression was also studied during saprotrophic and necrotrophic growth of the fungus. Three biological replicates were carried out for each treatment. As a control, *H. annosum s.s.* was grown in solid MEA at 20°C for two weeks. For saprotrophic growth, Scots pine sapwood was homogenized to powder form and autoclaved. Eight grams of the sapwood were mixed

with 8 ml of low nitrogen media (NH_4NO_3 0.6 g/L, K_2HPO_4 0.4 g/L, KH_2PO_4 0.5 g/L, $MgSO_4 \cdot 7H_2O$ 0.4 g/L) and 8 ml of sterile Milli-Q water. Three small agar blocks pre-colonized with *H. annosum s.s.* were placed in contact with the sapwood and incubated at 20°C in the dark for 3 months. Mycelia together with the sapwood were collected as saprotrophic samples. For necrotrophic growth, eleven-day-old Scots pine seedlings were placed on 1% water agar plates and roots were covered by cellophane pre-colonized with *H. annosum s.s.* Plates were kept in a growth chamber (12-h light/12-h dark photoperiod with 80% relative humidity at 24°C) for 15 days. Thereafter, cellophane was removed and infected roots were collected as necrotrophic samples. All samples were immediately frozen in liquid nitrogen followed by RNA extraction.

2.5 cDNA preparation, quantitative real-time PCR and data analysis

1 µg of each RNA sample was treated with DNase I (Thermo Scientific, Finland) and cDNA was synthesized by RevertAid Reverse Transcriptase (Thermo Scientific, Finland) according to the manufacturer's instructions. Primers were designed at the Roche Universal Probe Library Assay Design Center (http://www.roche-applied-science.com). Two technical replicates were carried out and each reaction was performed as follows: 5.5 µl cDNA (20-fold dilution), 1 µl forward primer (10 µM), 1 µl reverse primer (10 µM) and 7.5 µl Master-Mix (Roche, Finland).

A melting curve analysis was performed to assess primer' specificity and primer' efficiencies were calculated by using the Absolute Quantification/2nd Derivative Max method in the Light Cycler 480 II Software 1.5.1 (Supplementary Table 1). Primer' efficiencies were applied in the calculation of the relative expression level of each gene with the $2^{-\Delta\Delta Ct}$ method (Livak and Schmittgen, 2001). For cerato-platanin-like gene expression, both *Tryp Met* (*Tryptophan metabolism*) and *RNA Pol3 TF* (*RNA polymerase 3 transcription factor*) were used as reference genes (Raffaello and Asiegbu, 2013).

Statistical analysis of the qPCR data was assessed with one-way analysis of variance (ANOVA) followed by Tukey's multiple comparisons at 0.05 confidence level with GraphPad Prism software (GraphPad Software, Inc., USA).

2.6 Construction of a recombinant *Pichia pastoris* expression strain

The cDNA sequence of *hacpl2* without the secretion signal and stop codon was obtained by PCR using the Phusion DNA polymerase. The forward primer contained an *Xho I* restriction site and a KEX2 site, whereas the reverse primer contained an *Xba I* restriction site (Supplementary Table 1). The PCR product was then cloned into pPICZαA vector (Invitrogen) and verified by sequencing. The recombinant protein encoded by this construction contained the α-factor secretion signal from *Saccharomyces cerevisiae* at the *N*-terminus and the c-myc and 6×His epitopes at the *C*-terminus (Supplementary Fig. 3). The recombinant vector was linearized by *BstX I* restriction enzyme, purified by phenol:chloroform:isoamyl alcohol (25:24:1) extraction and transformed into *P. pastoris* X-33 strain by electroporation according to the EasySelect *Pichia* Expression Kit protocol (Invitrogen). Positive transformants X-33/pPICZαA/HaCPL2 were confirmed by colony PCR and phenotype was determined according to the EasySelect *Pichia* Expression Kit protocol. One of the transformants expressing HaCPL2 and one transformant of vector control X-33/pPICZαA (without *hacpl2* insert) were chosen for the subsequent work.

2.7 Expression, purification and identification of HaCPL2

The selected transformant was first cultured in BMGY (buffered complex glycerol medium) for 48 h and cells were harvested and re-suspended in BMMY (buffered complex methanol medium) to OD 3.5. Induction was carried out with methanol at a final concentration of 2% at 28°C with 250 rpm shaking for 5 days. With the aid of 6×His tag, the supernatant of the culture was used to purify

HaCPL2 with HisTrap^{TM} FF crude prepacked column (GE Healthcare, Finland) according to the manufacturer's instructions. Prior to loading the column, the supernatant was adjusted to pH 7.4 by addition of 4× binding buffer (80 mM sodium phosphate, 2 M NaCl, 80 mM imidazole, pH 7.4). The flow rate was 5 ml/min as recommended by the manufacturer's instructions. After washing with 1× binding buffer (20 mM sodium phosphate, 500 mM NaCl, 20 mM imidazole, pH 7.4), the protein was eluted by elution buffer (20 mM sodium phosphate, 500 mM NaCl, 500 mM imidazole, pH 7.4). The protein solution was then dialyzed against H_2O with high retention seamless cellulose tubing (MWCO 12400, Sigma-Aldrich, Finland) overnight at 4°C with two times water exchange in between. The dialyzed protein solution was then freeze-dried at –40°C overnight, re-suspended in nuclease-free water for desired concentration and stored at –80°C for further study. As a negative control for all further studies, X-33/pPICZαA (without *hacpl2* insert) was inoculated to the same media and the supernatant of the culture was purified in the same way as X-33/pPICZαA/HaCPL2 (referred as "vector" treatment in this paper).

Protein concentration was determined by Bradford method with a Nanodrop 2000C spectrophotometer (Thermo Scientific), using BSA as a standard. The presence of HaCPL2 was determined by sodium dodecyl sulfate-polyacrylamide gel (15%) electrophoresis (SDS-PAGE). The identification of the protein was carried out by Western-blot using anti-c-myc antibody produced in rabbit (Sigma-Aldrich, Finland) and MALDI-TOF-TOF mass spectrometry (Meilahti Clinical Proteomics Core Facility, University of Helsinki, Finland).

2.8 Infiltration of *N. tabacum* leaves with HaCPL2

5-week-old *N. tabacum* plants were used for infiltration. 60 µl of H_2O, vector (purification products from X-33/pPICZαA culture medium), BSA (1800 µg/ml), 38 µM (570 µg/ml) and or 120 µM

(1800 µg/ml) HaCPL2 was infiltrated to a young well-developed leaf with the aid of a syringe. The HaCPL2 solution used here and all subsequent studies was a mixture of different forms (monomer, dimer and polymer). Three biological replicates were performed and plants were kept in a growth room under controlled conditions (16-h light/8-h dark period with 80% relative humidity at 22°C).

2.9 Phytoalexin production induced by HaCPL2 in *N. tabacum* leaves

Leaf disks derived from a young well-developed leaf of a 5-week-old *N. tabacum* plant were placed in a 96-well plate followed by addition of 60 µl of H_2O, vector (purification products from X-33/pPICZαA culture medium), BSA (1800 µg/ml), 38 µM or 120 µM HaCPL2. The plate was kept shaking at 500 rpm at room temperature (22°C) under continuous light. Three replicates were performed and two time points (24 h and 48 h) were studied. After the incubation, solution from each treatment was collected and diluted to 500 µl with sterile water. Fluorescence was measured by PerkinElmer LS55 fluorospectrometer at the wavelengths of excitation 365 nm and emission 460 nm. 0.5 – 32 µM umbelliferone (Sigma-Aldrich, Finland) was used to prepare a standard curve and phytoalexin production was presented as umbelliferone equivalents. Statistical analysis was carried out with two-way analysis of variance (ANOVA) followed by Tukey's multiple comparisons at 0.05 confidence level with GraphPad Prism software.

2.10 Defense gene expression induced by HaCPL2 in *N. tabacum* leaves

N. tabacum leaves were infiltrated with 60 µl of H_2O or 120 µM HaCPL2. Three biological replicates were performed for each time point. Both control and protein-treated samples were harvested at 6 h, 12 h and 24 h after infiltration and frozen in liquid nitrogen followed by RNA isolation. cDNA synthesis and quantitative real-time PCR were carried out as described above (see section 2.5). Results were analyzed with the $2^{-\Delta\Delta Ct}$ method using *EF1α* (*Elongation factor 1 alpha*) as a reference gene.

Statistical analysis was assessed with unpaired t-test comparing to the control in each time point with GraphPad Prism software. Primers for the qPCR and their efficiencies were listed in Supplementary Table 1.

2.11 Infiltration of Scots pine seedlings with HaCPL2

Five-day-old Scots pine seedlings pre-germinated in 1% water agar plates were used for bioassay. Seedlings were moved to a new sterile Petri dish (diameter 140 mm) with 1% water agar and roots were placed in between two autoclaved filter paper stripes (30 mm × 7 mm). 60 and 40 µl of purified HaCPL2 was added evenly to the filter paper stripes below and above the seedling, respectively. Three concentrations of HaCPL2 were tested: 38 µM, 120 µM and 380 µM. Three negative controls were carried out: sterile H_2O, vector (purification products from X-33/pPICZαA culture medium) and BSA (1800 µg/ml). Instead of adding HaCPL2, 60 and 40 µl of sterile H_2O, vector and BSA was added evenly to the filter paper stripes below and above the seedling. As a positive control, roots of seedlings were placed on the filter paper stripes wetted with 60 µl of sterile H_2O and covered by cellophane pre-colonized by *H. annosum s.s.* Petri dishes were sealed with parafilm with the bottom section covered by aluminum foil and kept in the growth chamber (12-h light/12-h dark photoperiod with 80% relative humidity at 24°C) for 48 h. Three biological replicates were carried out and the positive control was performed in a separate Petri dish.

Necrosis symptoms were observed with stereomicroscope SteREO Discovery.V20 (Zeiss, Germany). Root length was measured before and after the treatments with ImageJ 1.48 software and statistical analysis was carried out with one-way analysis of variance (ANOVA) followed by Tukey's multiple comparisons at 0.05 confidence level with GraphPad Prism software.

2.12 Defense gene expression induced by HaCPL2 in Scots pine seedlings

Scots pine seedlings were treated with H_2O, 120 µM HaCPL2 or *H. annosum s.s.* as described above. Seedlings were harvested at 48 h after the treatments and frozen in liquid nitrogen followed by RNA isolation. cDNA synthesis and quantitative real-time PCR were carried out as described above (see section 2.5). Results were analyzed with the $2^{-\Delta\Delta Ct}$ method using *EF1α* (*Elongation factor 1 alpha*) as a reference gene. Statistical analysis was assessed with one-way analysis of variance (ANOVA) followed by Tukey's multiple comparisons at 0.05 confidence level with GraphPad Prism software. Primers for the qPCR and their efficiencies were listed in Supplementary Table 1.

2.13 Homology modeling

Similar protein structures to HaCPL2 deposited in the Protein Data Bank (PDB) (Altschul et al., 1997; Berman et al., 2000) were located using BLAST searches (Altschul et al., 1997), obtained, then superimposed and compared with the programs LSQMAN (Kleywegt et al., 2001) and O (Jones et al., 1991). The sequences of these structures and HaCPL2 were aligned using CLUSTAL W (Thompson et al., 1994). Based on the sequence identity, the homology model was built on the structure of *T. virens* Sm1 (PDB entry 3M3G; sequence identity 54%) in the program SOD (Kleywegt et al., 2001). The model was adjusted in O, using rotamers that would improve packing in the interior of the protein, and accounting for a deletion in a loop region. The figures were prepared using O, MOLSCRIPT (Kraulis, 1991), Molray (Harris and Jones, 2001) and PyMOL. Conserved residues were located using the multiple sequence alignment obtained from SAM_T02 server search (Karchin et al., 2003).

3. Results

3.1 HaCPL2 showed the highest sequence similarity to the reference protein cerato-platanin from *C. platani*

With the advantage of a published genome sequence from a closely related species *H. irregulare*, we were able to design gene-specific primers for the amplification of cerato-platanins from *H. annosum s.s.* The sequences of the three homologues obtained by using genomic DNA and cDNA as templates showed no difference, indicating there were no introns in these three genes (data not shown). *hacpl1*, *hacpl2* and *hacpl3* were 318 bp, 417 bp and 783 bp, encoding proteins of 105, 138 and 260 amino acids, respectively (GenBank accession numbers: *hacpl1* (KP288871), *hacpl2* (KP202174) and *hacpl3* (KP288872)). Both HaCPL2 and HaCPL3 contained a putative signal peptide of 19 amino acids predicted by SignalP 4.1, while no signal peptide was predicted in HaCPL1. All three proteins contained the cerato-platanin domain (IPR010829) and the four cysteine residues putatively involved in disulfide bridge formation were highly conserved, which defined this protein family (Supplementary Fig. 1). In terms of length, HaCPL2 showed the highest similarity to the reference protein cerato-platanin from *C. platani* (GenBank accession number: CAC84090.2), while HaCPL1 seemed to have an internal deletion of 15 amino acids in the *N*-terminal region and HaCPL3 had more than 100 extra amino acids in the *N*-terminal region characterized by low sequence complexity (Supplementary Fig. 1).

3.2 *hacpl2* was induced during nutrient starvation and necrotrophic growth

Our goal was to investigate whether cerato-platanins were involved in the interactions between *H. annosum s.s.* and Scots pine. Since three cerato-platanin-like genes showed considerable differences in the length of their sequences, it became imperative to study their expression profile before embarking on functional analysis. Expression of cerato-platanin-like genes under abiotic stress and during different nutrition modes was investigated by qRT-PCR. Interestingly, all of them were found to be induced during nutrient starvation, while no significant difference was found during osmotic or oxidative stress when compared to the control (Fig. 1A). Furthermore, *hacpl2* was significantly induced

during necrotrophic growth, 13 and 33 fold when compared to the expression in the control and saprotrophic growth, respectively (Fig. 1B).

3.3 Recombinant HaCPL2 existed as a mixture of different forms

Based on the sequence analysis and the expression profile of the three genes, *hacpl2* appeared to be the best candidate for functional characterization during the interactions between *H. annosum s.s.* and Scots pine. We performed recombinant overexpression of HaCPL2 in *P. pastoris*. The deduced recombinant protein sequence consisted of 227 amino acids including the *Saccharomyces cerevisiae* α-factor secretion signal peptide of 85 amino acids. The mature protein was expected to be 142 amino acid-long including a c-myc and a 6×His tag. The predicted molecular weight was 14943.48 Daltons and the isoelectric point was 4.56.

One positive *P. pastoris* transformant was chosen to express the recombinant HaCPL2. Different initial culture optical densities (OD), concentrations of methanol and induction time were tested to optimize the expression conditions. Results showed that the best expression was obtained when the culture was started at OD 3.5 and induced with 2% methanol (data not shown). The recombinant protein was induced and visible in SDS-PAGE gels after three days and was highly accumulated in the extracellular media at five days post induction (Fig. 2A). After purification on the HisTrap^{TM} FF crude column (GE Healthcare), the purity of the recombinant protein was assessed with SDS-PAGE and Western-blot analysis. Results indicated that the recombinant HaCPL2 existed as a mixture of different forms (monomer, dimer and polymer) (Fig. 2B) and this was confirmed by Western-blot (Fig. 2C) and mass spectrometry analysis (Supplementary Fig. 2). Two peptides (from amino acid 5 to 31 and 125 to 142) covering 31% of the mature protein were identified and matched the predicted mature protein sequence (data not shown). The spectrums of the three bands in Fig. 2B from MALDI-

TOF-TOF indicated that they corresponded to the same protein (Supplementary Fig. 2). Typically, the yield of pure recombinant HaCPL2 was about 16 mg from 1 L culture supernatant.

3.4 HaCPL2 induced cell death and phytoalexin production in *N. tabacum* leaves

In order to study the *in vivo* effect of the purified HaCPL2, a model plant, *N. tabacum*, a well-established system for elicitor and effector study, was assayed. Interestingly, HaCPL2 was able to induce cell death at the concentration of 120 µM but not 38 µM after infiltrated to *N. tabacum* leaves, indicating the threshold of the effect was between 38 and 120 µM. The symptoms started to appear three days after infiltration and continued to develop to a larger area for several days. A typical symptom of seven days after infiltration is shown in Fig 3A.

As a response to pest and pathogen attack, plants are able to produce low molecular mass secondary metabolites with antimicrobial activity, which are collectively known as phytoalexins (Ahuja et al., 2012). Therefore, phytoalexin production was measured before the cell death symptom development to study defense responses from *N. tabacum*. After 24 h incubation, the size and the stiffness of the leaf disks treated with120 µM HaCPL2 were reduced significantly and a slight discoloration was documented. After 48 h incubation, clear chlorotic symptoms suggesting loss of chlorophyll was observed for the leaf disks treated with 120 µM HaCPL2. A slight discoloration symptom was also observed for the leaf disks treated with 38 µM HaCPL2. However, no obvious symptoms were found for the other treatments (Fig. 3B). The phytoalexin production was also induced in a dose-dependent manner, which was well correlated to the severity of the symptoms displayed on the leaf disks. After 24 and 48 h, the phytoalexin production induced by 38 µM HaCPL2 was equivalent to approximately 2 nmol umbelliferone. An increase of phytoalexin production was observed for the treatment of 120 µM HaCPL2 between 24 and 48 h, equivalent to around 2 and 3 nmol umbelliferone,

respectively. In both time points, the production induced by 38 and 120 µM HaCPL2 was significantly higher than that in all control treatments (Fig. 3C). The two-way ANOVA analysis showed that the main factor for the significant differences was the treatment method rather than the time point (data not shown).

3.5 HaCPL2 induced defense gene expression in *N. tabacum* leaves

As cell death symptoms and phytoalexin production were induced by HaCPL2 when infiltrated to *N. tabacum* leaves, expression of genes related to plant defenses was also studied. The qRT-PCR results showed that in the early response phase (6 h after infiltration), *PR1a* (a marker of SA-mediated signaling pathway), *PAL* (phenylpropanoid pathway), *PR10* (a marker of hypersensitive cell death) and *PAD3* (camalexin biosynthesis pathway) were significantly up-regulated. Their expression remained at a higher level compared to the control after 12 h, except *PR1a*. After 24 h, *PR1a* expression increased while expression of *PAL* and *PR10* dropped to a similar level as the control. Only *PAD3* expression was induced significantly in all the time points. *PR2a* (a marker of SA-mediated signaling pathway) and *LOX* (JA-mediated signaling pathway) were induced only at a later time point of 24 h. However, a marker gene of ET-mediated signaling pathway *ERF1* was not induced in leaves treated with HaCPL2 (Fig. 4A). Another regulator gene related to JA-mediated signaling pathway *COI1* was significantly down-regulated in a time-dependent manner (Fig. 4B).

3.6 HaCPL2 induced necrosis and retarded the growth of Scots pine seedling roots

With the evidence that HaCPL2 was able to induce cell death and plant defense responses in non-host plant, this study was additionally conducted on its natural host (Scots pine). Three different concentrations of pure HaCPL2, three negative controls (H_2O, vector (purification products from X-33/pPICZαA culture medium), BSA) and one positive control (*H. annosum s.s.* infection) were used to

treat Scots pine seedling roots. Results showed that necrosis symptoms started to appear and root growth was delayed or retarded in the plants treated with 120 and 380 µM HaCPL2 and *H. annosum s.s.* after 24 h (data not shown). After 48 h, necrosis induced by 120 and 380 µM HaCPL2 was similar to that of *H. annosum s.s.* and the threshold of the effect was between 38 and 120 µM (Fig. 5A and B). The retardation of root growth was obvious, but interestingly, newly emerging apical root tips were also observed over time in the plants treated with 120 and 380 µM HaCPL2 (Fig. 5A and B). However, no necrosis was observed in the negative controls or with lower concentration of the protein (38 µM HaCPL2) (Fig. 5A and B). The growth of the roots at 48 h was significantly reduced in the treatment with 120 µM HaCPL2, 380 µM HaCPL2 and the positive control compared to the negative controls or lower concentration of the protein (Fig. 5C). However, no significant differences were observed for the growth of the upper part of the seedlings (Fig. 5A).

3.7 HaCPL2 induced defense gene expression in Scots pine seedlings

In order to investigate the defense responses underlying the necrotic reaction and retardation of the root growth, expression of several marker genes related to JA-mediated signaling pathway (*JAZ1*, *OPR* and *ERF1*), ET(*ACS* and *ERF1*) and terpene biosynthesis (*TPS*), cell wall modification (*PME* and *LAC*) and SA-mediated signaling pathway (*PAL1*, *NPR1* and *LURP1*) were studied. By including the positive control infected by *H. annosum s.s.*, we were able to compare whether a single protein was able to induce similar defense responses as the pathogen. Results showed that all the selected marker genes except for those related to SA-mediated signaling pathway were significantly up-regulated in the seedlings treated with HaCPL2 and *H. annosum s.s.* compared to the negative control, except for *JAZ1* and *ERF1* whose expressions in the protein treatment were not significantly higher than the negative control (Fig. 6).

3.8 Homology modeling

Protein functions and activities have a strong link to their structures. Since several necrosis-inducing cerato-platanins' structures were available, we performed homology modeling of HaCPL2. The model showed that HaCPL2 also has a double-ψβ-barrel fold as described for other cerato-platanins from filamentous fungi and expansins (Fig. 7A). The possible carbohydrate binding shallow surface is located in one side of the module with conserved amino acids (in gold). The conserved cysteine residues (in green) were responsible for the formation of two putative disulphide bonds (Fig. 7A).

4. Discussion

Cerato-platanins as well as elicitins, hydrophobins and some avirulence gene products are small, cysteine-rich proteins that are common among fungal secretomes and are involved in fungal development and interactions with plants (Templeton et al., 1994; Wosten, 2001; Pazzagli et al., 2014). They are specific for filamentous fungi in that no homologs are found in non-fungal species, early branches of jelly fungi or fungi with yeast or yeast-like forms in their life cycle (Chen et al., 2013). Recent gene duplications have been found in Basidiomycota which might indicate a higher functional diversity of this family in Basidiomycota than Ascomycota (Chen et al., 2013). In the conifer pathogen *H. annosum s.s.*, three cerato-platanin homologs were identified. However, only HaCPL2 and HaCPL3 contained a secretory signal peptide indicating that HaCPL1 might not be secreted or involved in the interactions with plants. Moreover, when compared to the reference protein cerato-platanin from *C. platani*, HaCPL1 seemed to be a truncated sequence and HaCPL3 had more than 100 extra amino acids in the *N*-terminal region with low sequence complexity. Only HaCPL2 showed high similarity to the reference protein in terms of length and secretion signal. Despite the sequence diversity, all cerato-

platanin-like genes were significantly induced during nutrient starvation. Under this condition, only limited amount of carbon was supplied in the form of 0.2 g/L glucose in water with complete deprivation of nitrogen. Our results thus indicate that HaCPLs from *H. annosum s.s.* might be involved in overcoming starving conditions. The cerato-platanin gene *MSP1* from *Magnaporthe grisea* is also induced upon nitrogen starvation which mimics the environment *in planta* (Jeong et al., 2007). Both nutrient starvation and the adverse environment created by plants in the host-pathogen interface can induce gene expression related to autophagy, an adaptive strategy under stressful stimuli (Deng et al., 2012; Raffaello et al., 2014). Moreover, only *hacpl2* was induced during necrotrophic growth, reflecting that HaCPL2 might be involved in the interactions between the fungus and living plants. This is similar to the observations for some cerato-platanin proteins from other pathogens. For instance, *SnodProt1* from *Stagonospora nodorum* and *sp1* from *Leptosphaeria maculans* are induced during infection (Hall et al., 1999; Wilson et al., 2002). *MSP1* from *M. grisea* is induced during appressorium formation (Jeong et al., 2007). *Sm1* from *T. virens*, *MpCP1* from *M. perniciosa* and *BcSpl1 B. cinerea* are induced in the presence of plant hosts (Djonovic et al., 2006; Zaparoli et al., 2009; Frias et al., 2011). Consequently, HaCPL2 was chosen for further study about the virulence determinants in the *H.annosum s.s.-P. sylvestris* pathosystem.

Due to the low efficiency in constructing a stable gene-specific mutant in *H. annosum s.s.* (Samils et al., 2006), heterologous expression in *P. pastoris* was applied to obtain pure HaCPL2 for functional characterization. As a eukaryote, the *P. pastoris* expression system has many advantages such as proper protein processing, folding, post-translational modification and generally gives a satisfactory expression level of target proteins (Li et al., 2007). In this study, the yield of pure HaCPL2 increased with incubation time and reached an optimal level, around 16 mg from 1 L culture medium after five days. This is comparable to the values documented in other studies using *P. pastoris* to express cerato-

platanins. From 1 L culture medium, the yield of cerato-platanin from *C. platani*, Sm1 from *T. virens*, BcSpl1 from *B. cinerea* are 32, 55 and 35 mg, respectively (Carresi et al., 2006; Buensanteai et al., 2010; Frias et al., 2011). Pure HaCPL2 existed as a mixture of different forms (monomer, dimer and polymer), similarly to other cerato-platanins (monomer and aggregate forms in *C. platani*, monomer and dimer in *T. virens* and *Trichoderma atroviride*, monomer and trimer in *Trichoderma reesei* and monomer, dimer and trimer in *M. grisea*) (Vargas et al., 2008). In *T. virens*, the eliciting ability of Sm1 has been found to be controlled by dimerization with only monomeric form able to induce systemic resistance in plants and glycosylation is the key factor that prevents dimerization of Sm1 (Vargas et al., 2008).

Members of the cerato-platanin family display functional diversity with distinctive regulatory patterns suggesting different roles in fungal life style. For instance, *Snodprot1* from *Neurospora crassa* is a clock-controlled gene and *SP1* from *L. maculans* is light-regulated (Zhu et al., 2001; Wilson et al., 2002). However, the eliciting ability seems to be a common characteristic of this protein family. They are able to induce immune responses in both animals and plants. CS-AG from *Coccidioides immitis* is an antigen and rAsp f 13 of *Aspergillus fumigatus* is an allergen to humans (Pan and Cole, 1995; Chaudhary et al., 2010). Cerato-platanins from genus *Trichoderma* such as Epl1 from *T. atroviride* and Sm1 from *T. virens* have been found to act as elicitors, without necrosis-inducing ability (Djonovic et al., 2006; Seidl et al., 2006; Djonovic et al., 2007). Nevertheless, cerato-platanins from some pathogens, such as CP from *C. platani*, MSP1 from *M. grisea*, Pop1 from *Ceratocystis populicola*, MpCP1 from *M. perniciosa* and BcSpl1 from *B. cinerea*, are able to induce necrosis, programmed cell death or different plant defense responses (Pazzagli et al., 1999; Scala et al., 2004; Jeong et al., 2007; Comparini et al., 2009; Zaparoli et al., 2009; Frias et al., 2011). In this study, we demonstrated that cerato-platanin-like protein HaCPL2 from a necrotrophic basidiomycete pathogen *H. annosum s.s.* was able to cause cell death and activate defense responses in host and non-host plants. In other studies,

cerato-platanin from *C. platani*, MpCP1 from *M. perniciosa* and BcSpl1 from *B. cinerea* have been shown to induce plant cell death at the concentration of 80, 29 and 34 µM respectively but not at lower concentration (Pazzagli et al., 1999; Zaparoli et al., 2009; Frias et al., 2011). Therefore, the inability to cause cell death at 38 µM of HaCPL2 suggests that its phytotoxicity might be strongly related to its concentration and the threshold of the cell death-inducing effect could be between 38 and 120 µM. In line with our observations, *MSP1* from *M. grisea* and BcSpl1 from *B. cinerea* have been reported to be required for full virulence of the pathogens (Jeong et al., 2007; Frias et al., 2011). Besides necrotic symptoms, growth of the Scots pine seedling roots was retarded after HaCPL2 treatment. This might indicate a physiological switch from a growth to a defense program in the plant (Boller and Felix, 2009). Since *H. annosum s.s.* is a necrotrophic pathogen, it normally kills living cells before colonization and feeds on dead tissues (Asiegbu et al., 2005). Interestingly, the *in planta* effect induced by HaCPL2 is similar to that caused by the pathogen. Therefore, it suggests that HaCPL2 might be one of the molecules that *H. annosum s.s.* exploits as weapons to induce cell death on its host in order to promote tissue colonization and invasive growth. This effect on conifer seedlings has not been observed before and thus constitutes a step forward towards the elucidation of the role of HaCPLs in disease development.

It is widely accepted that plants have developed two layers of innate immunity against pathogen attack, PAMP-triggered immunity (PTI) and effector-triggered immunity (ETI) (Jones and Dangl, 2006). PTI is activated by the recognition of Pathogen Associated Molecular Patterns (PAMPs) by pattern recognition receptors (PRR) and ETI is highly specific and mediated by direct or indirect interaction of pathogen effectors and products of plant *R* genes according to the gene-for-gene theory (Boller and Felix, 2009). In this study, HaCPL2 was able to induce defense responses in both host and non-host plants. Many small cysteine-rich proteins have been identified as apoplastic effectors, such as

Phytophthora elicitins, *Cladosporium fulvum Avr2*, *Avr4* and *Avr9*, *Rhynchosporium secalis nip1* and *S. nodorum SnTox1* (Vandenackerveken et al., 1992; Rohe et al., 1995; Sasabe et al., 2000; van Esse et al., 2007; van Esse et al., 2008; Liu et al., 2012). It seems reasonable to hypothesize that HaCPL2 could act as an avirulence factor or a phytotoxic protein. Responses to both PTI and ETI include rapid influx of calcium ions, oxidative burst, activation of MAPKs, changes in protein phosphorylation, hormone biosynthesis, phytoalexin biosynthesis, the reinforcement of cell walls at the site of attempted infection, receptor endocytosis and transcriptional reprogramming (Schwessinger and Zipfel, 2008; Segonzac and Zipfel, 2011). During infection, not only changes in secondary metabolism are promoted to activate defense responses, but also in primary metabolism, with reduced growth and abnormal development in many cases (Berger et al., 2007). In this study, HaCPL2 was able to induce phytoalexin synthesis and defense gene expression in the model plant *N. tabacum*. In other studies, cerato-platanin from *C. platani*, *sp1* from *L. maculans*, Sm1 from *T. virens* and Pop1 from *C. populicola* are also able to induce phytoalexin production or autofluorescence in the plant tissues (Pazzagli et al., 1999; Wilson et al., 2002; Scala et al., 2004; Djonovic et al., 2006; Comparini et al., 2009). Other plant responses, such as accumulation of reactive oxygen species and transcriptional activation of defense genes, have also been reported to be induced by cerato-platanin family proteins (Djonovic et al., 2006; Frias et al., 2011). Interestingly, HaCPL2 retarded root growth and induced defense gene expression in Scots pine seedlings. Both early (transcriptional activation) and late (growth inhibition) responses were observed in the host plant after treatment with HaCPL2 and *H. annosum s.s*. The similar responses induced by HaCPL2 and the pathogen on Scots pine seedlings indicates the host might perceive the presence of HaCPL2 as a signal of pathogen invasion and subsequently activate defense machinery.

The downstream responses to both PTI and ETI are controlled by the balanced action of salicylic acid (SA), jasmonic acid (JA) and ethylene (ET) (Bari and Jones, 2009; Robert-Seilaniantz et

al., 2011). It has been established that JA and ET-dependent responses are involved in the plant defenses against necrotrophic pathogens and insect damage, while SA-dependent defenses are often triggered by biotrophic pathogens (Spoel et al., 2007). In *N. tabacum*, the up-regulation of SA-dependent marker genes *PR1a*, *PR2a* and *PR10* is congruent with the activation of SA-mediated signaling pathway after treatment with HaCPL2 (Jwa et al., 2001; Jia et al., 2013; Kim and Hwang, 2014). *PAL* accumulation contributes to this assumption, since the corresponding gene product acts as a positive regulator of SA-dependent defense signaling to combat microbial pathogens (Kim and Hwang, 2014). These results in *N. tabacum* agree with the observations that infiltration of BcSpl1 from *B. cinerea* leads to the accumulation of SA in tobacco leaves (Frias et al., 2013). Moreover, *PR10* is a marker gene for HR-induced cell death, which supports our *in vivo* observations (Choi et al., 2012). The up-regulation of *LOX* and down-regulation of *COI1* suggest that JA-dependent defense gene expression might be promoted by HaCPL2 treatment. COI1 mediates JA-mediated signaling pathway by promoting hormone-dependent ubiquitylation and degradation of transcriptional repressor JAZ proteins (Schaller and Stintzi, 2009; Sheard et al., 2010). Therefore, we hypothesize that JAZ proteins are accumulated, acting as transcriptional repressors by interacting with MYC2 and promoting the defense-related gene expression (ERF branch of JA signaling) over wounding-related response (MYC branch of JA signaling) (Lorenzo et al., 2004; Fernandez-Calvo et al., 2011). The up-regulation of *PAL* is in agreement with accumulation of phytoalexins. After pathogen challenge, the phenylpropanoid pathway is redirected towards the synthesis of phytoalexins and other defensive secondary metabolites (Vogt, 2010). Increased mRNA transcripts of *PAD3*, a gene encoding for a key enzyme in camalexin biosynthesis, was also consistent with the activation of phytoalexin production (Zhou et al., 1999). In Scots pine seedlings, the JA-dependent marker genes *JAZ1* and *OPR* were significantly induced after both HaCPL2 treatment and challenge with *H. annosum s.s.*, suggesting JA-mediated signaling pathway might be activated (Schaller

and Stintzi, 2009; Sheard et al., 2010). Additionally, the induction of *ACS* and *ERF1* suggests that JA and ET act concomitantly to control defense responses through the ERF branch of JA/ET synergistic pathway. This branch of transcriptional regulation is known to be preferentially induced by necrotrophic pathogens (Lorenzo et al., 2004). Furthermore, *TPS*, *PME* and *LAC*, encoding for enzymes implicated in biosynthesis of terpenes, cell wall modification or lignification, are induced (Micheli, 2001; Tholl, 2006; Berthet et al., 2012). *PAL1*, *NPR1* (a positive regulator of SA signal transduction) or *LURP1* (required for full basal defenses against pathogens) were not differentially expressed, so no evidence was found for induction of SA-dependent defenses or the phenylpropanoid pathway (Asai et al., 2000; Knoth and Eulgem, 2008). In *Arabidopsis thaliana*, cerato-platanin from *C. platani* has been found to induce camalexin biosynthesis and defenses mediated by SA and ET (Baccelli et al., 2014a). Nonetheless, the results in Scots pine are congruent with the induction of JA/ET-mediated signaling pathways after infection with necrotrophic pathogens (Zhu et al., 2011).

Small cysteine rich effectors usually consist of less than 150 amino acids and contain a secretion signal and an even number of disulfide bridge-forming cysteine residues that are essential for defense induction and effector function when infiltrated into plant tissues (Joosten et al., 1997; Kooman-Gersmann et al., 1997; Lauge and De Wit, 1998; Kamoun et al., 1999; Luderer et al., 2002; van't Slot and Knogge, 2002). HaCPL2 contains 119 amino acids, a secretion signal and 4 cysteine residues, which matches all these characteristics. Moreover, the predicted protein structure of HaCPL2 also has a double-ψβ-barrel fold similar to other cerato-platanins and expansins (de Oliveira et al., 2011). Cerato-platanin locates in the fungal cell wall and is able to bind to chitin (de Oliveira et al., 2011; Frischmann et al., 2013; Baccelli et al., 2014b; Frias et al., 2014). It has been suggested that cerato-platanin proteins can act on non-covalent interactions both in cellulose- and chitin-containing cell walls reducing the force needed to break the plant cell walls. Therefore, binding of cerato-platanin provides mechanical pressure

assisting the penetration of hyphae (Baccelli, 2015). BcSpl1 of *B. cinerea* binds to plasma membrane and causes cell shrinkage and chloroplast disorganization. Mutational studies reveal two motifs contributing to the necrosis-inducing ability of BcSpl1 (Frias et al., 2014). These motifs are fairly conserved in HaCPL2 and possibly contribute to chitin binding as well as the stability of the structure. Close observation of the homology model also reveals that some of these conserved residues are surface exposed, possibly having implication for carbohydrate binding. The homology modeling might assist further studies to explain the eliciting and necrosis-inducing ability of HaCPL2. As one of the most economically important forest pathogens, *H. annosum s.s.* presents an epidemiologically well-studied fungus with a complex life style. The ability to switch the life style between saprotrophic and necrotrophic phases requires the pathogen to be able to kill living tissues or cause necrotic cell death so that it can feed on the dead tissue. In the *H. annosum s.s.-P. sylvestris* pathosystem, we have purified and characterized a cerato-platanin protein that induces cell death and plant defense responses. This will further our understanding of the determinants of pathogenicity or virulence as well as provide a possible target for disease control in the future.

Acknowledgements

This work was supported by the Academy of Finland. Supports from Integrative Life Science Doctoral Program (ILS) to Hongxin Chen are gratefully acknowledged. We thank Professor Yong-Hwan Lee and Docent Minna Rajamäki for all the ideas and supports during the study.

References

Ahuja, I., et al., 2012. Phytoalexins in defense against pathogens. Trends in Plant Science. 17**,** 73–90.

Altschul, S. F., et al., 1997. Gapped BLAST and PSI-BLAST: a new generation of protein database search programs. Nucleic Acids Research. 25**,** 3389–3402.

Asai, T., et al., 2000. Fumonisin B1-induced cell death in *Arabidopsis* protoplasts requires jasmonate-, ethylene-, and salicylate-dependent signaling pathways. Plant Cell. 12**,** 1823–1835.

Asiegbu, F. O., et al., 2005. Conifer root and butt rot caused by *Heterobasidion annosum* (Fr.) Bref. *s.l.* Molecular Plant Pathology. 6**,** 395–409.

Baccelli, I., et al., 2012. The expression of the cerato-platanin gene is related to hyphal growth and chlamydospores formation in *Ceratocystis platani*. FEMS Microbiology Letters. 327**,** 155–163.

Baccelli, I., et al., 2014a. Cerato-platanin induces resistance in *Arabidopsis* leaves through stomatal perception, overexpression of salicylic acid- and ethylene-signalling genes and camalexin biosynthesis. Plos One. 9.

Baccelli, I., 2015. Cerato-platanin family proteins: one function for multiple biological roles? Frontiers in Plant Science. 5.

Baccelli, I., et al., 2014b. Cerato-platanin shows expansin-like activity on cellulosic materials. Applied Microbiology and Biotechnology. 98**,** 175–184.

Bari, R., Jones, J., 2009. Role of plant hormones in plant defence responses. Plant Molecular Biology. 69**,** 473–488.

Berger, S., et al., 2007. Plant physiology meets phytopathology: plant primary metabolism and plant-pathogen interactions. Journal of Experimental Botany. 58**,** 4019–4026.

Berman, H. M., et al., 2000. The Protein Data Bank. Nucleic Acids Research. 28**,** 235–242.

Berthet, S., et al., 2012. Role of Plant Laccases in Lignin Polymerization. Lignins: Biosynthesis, Biodegradation and Bioengineering. 61**,** 145–172.

Boddi, S., et al., 2004. Cerato-platanin protein is located in the cell walls of ascospores, conidia and hyphae of *Ceratocystis fimbriata* f. sp *platani*. FEMS Microbiology Letters. 233**,** 341–346.

Boller, T., Felix, G., 2009. A renaissance of elicitors: perception of microbe-associated molecular patterns and danger signals by pattern-recognition receptors. Annual Review of Plant Biology. 60**,** 379–406.

Buensanteai, N., et al., 2010. Expression and purification of biologically active *Trichoderma virens* proteinaceous elicitor Sm1 in *Pichia pastoris*. Protein Expression and Purification. 72**,** 131–138.

Caarls, L., et al., 2015. How salicylic acid takes transcriptional control over jasmonic acid signaling. Frontiers in Plant Science. 6.

Carresi, L., et al., 2006. Cerato-platanin, a phytotoxic protein from *Ceratocystis fimbriata*: Expression in *Pichia pastoris*, purification and characterization. Protein Expression and Purification. 49**,** 159–167.

Chaudhary, N., et al., 2010. Healthy human T-Cell responses to *Aspergillus fumigatus* antigens. Plos One. 5.

Chen, H., et al., 2013. Distribution and bioinformatic analysis of the cerato-platanin protein family in Dikarya. Mycologia. 105**,** 1479–1488.

Choi, D. S., et al., 2012. Requirement of the cytosolic interaction between pathogenesis-related protein 10 and leucine-rich repeat protein1 for cell death and defense signaling in pepper. Plant Cell. 24**,** 1675–1690.

Comparini, C., et al., 2009. New proteins orthologous to cerato-platanin in various *Ceratocystis* species and the purification and characterization of cerato-populin from *Ceratocystis populicola*. Applied Microbiology and Biotechnology. 84**,** 309–322.

Dai, Y. C., Korhonen, K., 1999. *Heterobasidion annosum* group S identified in north-eastern China. European Journal of Forest Pathology. 29**,** 273–279.

Dai, Y. C., et al., 2003. Investigations on *Heterobasidion annosum s. lat.* in central and eastern Asia with the aid of mating tests and DNA fingerprinting. Forest Pathology. 33**,** 269–286.

de O. Barsottini, M. R., et al., 2013. Functional diversification of cerato-platanins in *Moniliophthora perniciosa* as seen by differential expression and protein function specialization. Molecular Plant-Microbe Interactions. 26**,** 1281–1293.

de Oliveira, A. L., et al., 2011. The structure of the elicitor cerato-platanin (CP), the first member of the CP fungal protein family, reveals a double ψβ-barrel fold and carbohydrate binding. The Journal of Biological Chemistry. 286**,** 17560–17568.

Deng, Y., et al., 2012. Role of macroautophagy in nutrient homeostasis during fungal development and pathogenesis. Cells. 1**,** 449–463.

Djonovic, S., et al., 2006. Sm1, a proteinaceous elicitor secreted by the biocontrol fungus *Trichoderma virens* induces plant defense responses and systemic resistance. Molecular Plant-Microbe Interactions. 19**,** 838–853.

Djonovic, S., et al., 2007. A proteinaceous elicitor Sm1 from the beneficial fungus *Trichoderma virens* is required for induced systemic resistance in maize. Plant Physiology. 145**,** 875–889.

Fernandez-Calvo, P., et al., 2011. The *Arabidopsis* bHLH transcription factors MYC3 and MYC4 are targets of JAZ repressors and act additively with MYC2 in the activation of jasmonate responses. Plant Cell. 23**,** 701–715.

Frias, M., et al., 2011. BcSpl1, a cerato-platanin family protein, contributes to *Botrytis cinerea* virulence and elicits the hypersensitive response in the host. New phytologist. 192**,** 483–495.

Frias, M., et al., 2013. The *Botrytis cinerea* cerato-platanin BcSpl1 is a potent inducer of systemic acquired resistance (SAR) in tobacco and generates a wave of salicylic acid expanding from the site of application. Molecular Plant Pathology. 14**,** 191–196.

Frias, M., et al., 2014. The phytotoxic activity of the cerato-platanin BcSpl1 resides in a two-peptide motif on the protein surface. Molecular Plant Pathology. 15, 342–351.

Frischmann, A., et al., 2013. Self-assembly at air/water interfaces and carbohydrate binding properties of the small secreted protein EPL1 from the fungus *Trichoderma atroviride*. Journal of Biological Chemistry. 288**,** 4278–4287.

Garbelotto, M., Gonthier, P., 2013. Biology, epidemiology, and control of *Heterobasidion* species worldwide. Annual Review of Phytopathology. 51**,** 39–59.

Hall, N., et al., 1999. A homologue of a gene implicated in the virulence of human fungal diseases is present in a plant fungal pathogen and is expressed during infection. Physiological and Molecular Plant Pathology. 55**,** 69–73.

Harris, M., Jones, T. A., 2001. Molray - a web interface between O and the POV-Ray ray tracer. Acta Crystallographica Section D-Biological Crystallography. 57**,** 1201–1203.

Jeong, J. S., et al., 2007. The *Magnaporthe grisea* snodprot1 homolog, MSP1, is required for virulence. FEMS Microbiology Letters. 273**,** 157–165.

Jia, C. G., et al., 2013. Multiple phytohormone signalling pathways modulate susceptibility of tomato plants to *Alternaria alternata* f. sp *lycopersici*. Journal of Experimental Botany. 64**,** 637–650.

Jones, J. D. G., Dangl, J. L., 2006. The plant immune system. Nature. 444**,** 323–329.

Jones, T. A., et al., 1991. Improved Methods for Building Protein Models in Electron-Density Maps and the Location of Errors in These Models. Acta Crystallographica Section A. 47**,** 110–119.

Joosten, M. H. A. J., et al., 1997. The biotrophic fungus *Cladosporium fulvum* circumvents Cf-4-mediated resistance by producing unstable AVR4 elicitors. Plant Cell. 9**,** 367–379.

Jwa, N. S., et al., 2001. Molecular cloning and characterization of a novel jasmonate inducible pathogenesis-related class 10 protein gene, *JIOsPR10,* from rice (*Oryza sativa* L.) seedling leaves. Biochemical and Biophysical Research Communications. 286**,** 973–983.

Kamoun, S., et al., 1999. The fungal gene *AVR9* and the oomycete gene *inf1* confer avirulence to potato virus X on tobacco. Molecular Plant-Microbe Interactions. 12**,** 459–462.

Karchin, R., et al., 2003. Hidden Markov models that use predicted local structure for fold recognition: Alphabets of backbone geometry. Proteins-Structure Function and Bioinformatics. 51**,** 504–514.

Kim, D. S., Hwang, B. K., 2014. An important role of the pepper phenylalanine ammonia-lyase gene (*PAL1*) in salicylic acid-dependent signalling of the defence response to microbial pathogens. Journal of Experimental Botany. 65**,** 2295–2306.

Kleywegt, G. J., et al., 2001. International Tables for Crystallography. Springer Netherlands.

Knoth, C., Eulgem, T., 2008. The oomycete response gene *LURP1* is required for defense against *Hyaloperonospora parasitica* in *Arabidopsis thaliana*. Plant Journal. 55**,** 53–64.

Kooman-Gersmann, M., et al., 1997. Assignment of amino acid residues of the AVR9 peptide of *Cladosporium fulvum* that determine elicitor activity. Molecular Plant-Microbe Interactions. 10**,** 821–829.

Kraulis, P. J., 1991. Molscript - a Program to Produce Both Detailed and Schematic Plots of Protein Structures. Journal of Applied Crystallography. 24**,** 946–950.

Lauge, R., De Wit, P. J. G. M., 1998. Fungal avirulence genes: structure and possible functions. Fungal Genetics and Biology. 24**,** 285–297.

Li, P. Z., et al., 2007. Expression of recombinant proteins in *Pichia pastoris*. Applied Biochemistry and Biotechnology. 142**,** 105–124.

Liu, Z. H., et al., 2012. The cysteine rich necrotrophic effector SnTox1 produced by *Stagonospora nodorum* triggers susceptibility of wheat lines harboring Snn1. Plos Pathogens. 8.

Livak, K. J., Schmittgen, T. D., 2001. Analysis of relative gene expression data using real-time quantitative PCR and the $2^{-\Delta\Delta Ct}$ method. Methods. 25**,** 402–408.

Lorenzo, O., et al., 2004. *Jasmonate-insensitive1* encodes a MYC transcription factor essential to discriminate between different jasmonate-regulated defense responses in *Arabidopsis*. Plant Cell. 16**,** 1938–1950.

Luderer, R., et al., 2002. Functional analysis of cysteine residues of ECP elicitor proteins of the fungal tomato pathogen *Cladosporium fulvum*. Molecular Plant Pathology. 3**,** 91–95.

Micheli, F., 2001. Pectin methylesterases: cell wall enzymes with important roles in plant physiology. Trends in Plant Science. 6**,** 414–419.

Pan, S. C., Cole, G. T., 1995. Molecular and biochemical characterization of a *Coccidioides immitis*-specific antigen. Infection and Immunity. 63**,** 3994–4002.

Pazzagli, L., et al., 1999. Purification, characterization, and amino acid sequence of cerato-platanin, a new phytotoxic protein from *Ceratocystis fimbriata* f. sp *platani*. Journal of Biological Chemistry. 274**,** 24959–24964.

Pazzagli, L., et al., 2014. Cerato-platanins: elicitors and effectors. Plant Science. 228**,** 79–87.

Raffaello, T., Asiegbu, F., 2013. Evaluation of potential reference genes for use in gene expression studies in the conifer pathogen (*Heterobasidion annosum*). Molecular biology reports. 40, 1–7.

Raffaello, T., et al., 2012. Role of the HaHOG1 MAP kinase in response of the conifer root and butt rot pathogen (*Heterobasidion annosum*) to osmotic and oxidative stress. Plos One. 7.

Raffaello, T., et al., 2014. Transcriptomic profiles of *Heterobasidion annosum* under abiotic stresses and during saprotrophic growth in bark, sapwood and heartwood. Environmental Microbiology. 16**,** 1654–1667.

Robert-Seilaniantz, A., et al., 2011. The microRNA miR393 re-directs secondary metabolite biosynthesis away from camalexin and towards glucosinolates. Plant Journal. 67**,** 218–231.

Rohe, M., et al., 1995. The race-specific elicitor, Nip1, from the barley pathogen, *Rhynchosporium Secalis*, determines avirulence on host plants of the Rrs1 resistance genotype. Embo Journal. 14, 4168–4177.

Samils, N., et al., 2006. Development of a rapid and simple *Agrobacterium tumefaciens*-mediated transformation system for the fungal pathogen *Heterobasidion annosum*. FEMS Microbiology Letters. 255, 82–88.

Sasabe, M., et al., 2000. Independent pathways leading to apoptotic cell death, oxidative burst and defense gene expression in response to elicitin in tobacco cell suspension culture. European Journal of Biochemistry. 267, 5005–5013.

Scala, A., et al., 2004. Cerato-platanin, an early-produced protein by *Ceratocystis fimbriata* f.sp. *platani*, elicits phytoalexin synthesis in host and non-host plants. Journal of Plant Pathology. 86**,** 27–33.

Schaller, A., Stintzi, A., 2009. Enzymes in jasmonate biosynthesis - structure, function, regulation. Phytochemistry. 70**,** 1532–1538.

Schwessinger, B., Zipfel, C., 2008. News from the frontline: recent insights into PAMP-triggered immunity in plants. Current Opinion in Plant Biology. 11**,** 389–395.

Segonzac, C., Zipfel, C., 2011. Activation of plant pattern-recognition receptors by bacteria. Current Opinion in Microbiology. 14**,** 54–61.

Seidl, V., et al., 2006. Epl1, the major secreted protein of *Hypocrea atroviridis* on glucose, is a member of a strongly conserved protein family comprising plant defense response elicitors. FEBS Journal. 273**,** 4346–4359.

Sheard, L. B., et al., 2010. Jasmonate perception by inositol-phosphate-potentiated COI1-JAZ co-receptor. Nature. 468**,** 400–405.

Spoel, S. H., et al., 2007. Regulation of tradeoffs between plant defenses against pathogens with different lifestyles. Proceedings of the National Academy of Sciences of the United States of America. 104**,** 18842–18847.

Templeton, M. D., et al., 1994. Small, cysteine-rich proteins and recognition in fungal-plant interactions. Molecular Plant-Microbe Interactions. 7**,** 320–325.

Tholl, D., 2006. Terpene synthases and the regulation, diversity and biological roles of terpene metabolism. Current Opinion in Plant Biology. 9**,** 297–304.

Thompson, J. D., et al., 1994. Clustal-W: improving the sensitivity of progressive multiple sequence alignment through sequence weighting, position-specific gap penalties and weight matrix choice. Nucleic Acids Research. 22**,** 4673–4680.

Vandenackerveken, G. F. J. M., et al., 1992. Molecular analysis of the avirulence gene *Avr9* of the fungal tomato pathogen *Cladosporium-Fulvum* fully supports the gene-for-gene hypothesis. Plant Journal. 2, 359–366.

van Esse, H. P., et al., 2007. The chitin-binding *Cladosporium fulvum* effector protein Avr4 is a virulence factor. Molecular Plant-Microbe Interactions. 20, 1092–1101.

van Esse, H. P., et al., 2008. The *Cladosporium fulvum* virulence protein Avr2 inhibits host proteases required for basal defense. Plant Cell. 20, 1948–1963.

van't Slot, K. A. E., Knogge, W., 2002. A dual role for microbial pathogen-derived effector proteins in plant disease and resistance. Critical Reviews in Plant Sciences. 21**,** 229–271.

Vargas, W. A., et al., 2008. Dimerization controls the activity of fungal elicitors that trigger systemic resistance in plants. Journal of Biological Chemistry. 283**,** 19804–19815.

Vogt, T., 2010. Phenylpropanoid Biosynthesis. Molecular Plant. 3, 2–20.

Waterhouse, A. M., et al., 2009. Jalview Version 2 – a multiple sequence alignment editor and analysis workbench. Bioinformatics. 25**,** 1189–1191.

Wilson, L. M., et al., 2002. Characterization of a gene (*sp1*) encoding a secreted protein from *Leptosphaeria maculans*, the blackleg pathogen of *Brassica napus*. Molecular Plant Pathology. 3**,** 487–493.

Wosten, H. A. B., 2001. Hydrophobins: multipurpose proteins. Annual Review of Microbiology. 55**,** 625–646.

Zaparoli, G., et al., 2009. Identification of a second family of genes in *Moniliophthora perniciosa*, the causal agent of witches' broom disease in cacao, encoding necrosis-inducing proteins similar to cerato-platanins. Mycological Research. 113**,** 61–72.

Zhou, N., et al., 1999. *Arabidopsis PAD3*, a gene required for camalexin biosynthesis, encodes a putative cytochrome P450 monooxygenase. Plant Cell. 11**,** 2419–2428.

Zhu, H., et al., 2001. Analysis of expressed sequence tags from two starvation, time-of-day-specific libraries of *Neurospora crassa* reveals novel clock-controlled genes. Genetics. 157**,** 1057–1065.

Zhu, Z. Q., et al., 2011. Derepression of ethylene-stabilized transcription factors (EIN3/EIL1) mediates jasmonate and ethylene signaling synergy in *Arabidopsis*. Proceedings of the National Academy of Sciences of the United States of America. 108**,** 12539–12544.

Fig. 1. Expression profile of cerato-platanin-like genes by RT-qPCR. A, gene expression under different abiotic stress. B, gene expression during different growth stages. Results were presented as fold change in amount of transcript levels compared to the control (±SEM, n=3). Lower case letters above the bars represented the statistical analysis assessed with one-way analysis of variance (ANOVA) within the same gene and followed by Tukey's multiple comparisons at 0.05 confidence level.

Fig. 2. Expression, purification and identification of recombinant protein HaCPL2. A, SDS-PAGE analysis of the time-course study of the production of recombinant HaCPL2 in the supernatant of the culture. 0 – 5d represented time points from 0 to 5 days, respectively. M: (the same in A, B and C) PageRuler Plus Prestained Protein Ladder (Thermo Scientific). B, SDS-PAGE analysis of the purified recombinant HaCPL2. Three bands indicated by the arrows were sent for identification with MALDI-TOF-TOF. C, Western-blot analysis of the recombinant HaCPL2 by using anti-c-myc antibody.

Fig. 3. Infiltration of HaCPL2 on *N. tabacum* leaves and phytoalexin production induced by HaCPL2. A, cell death induced by HaCPL2 seven days after infiltration. B, *N. tabacum* leaf disks after 24 and 48 h incubation with HaCPL2 in a 96-well plate. C, phytoalexin production induced by HaCPL2 after 24 and 48 h incubation. Values were presented as umbelliferone equivalents. Lower case letters above the bars represented the statistical analysis of two-way analysis of variance (ANOVA) followed by Tukey's multiple comparisons at 0.05 confidence level (±SEM, n=3).

Fig. 4. Defense gene expression induced by HaCPL2 in *N. tabacum* leaves by RT-qPCR. Results were presented as fold change in amount of transcript levels compared to the control in each time point, respectively (±SEM, n=3). A, defense genes that were up-regulated by HaCPL2. *PR1a*: *Pathogenesis related protein 1a*, *PR2a*: *Pathogenesis related protein 2a*, *PAL*: *Phenylalanine ammonia lyase*, *PR10*: *Pathogenesis related protein 10*, *LOX*: *Lipoxygenase*, *PAD3*: *Phytoalexin deficient 3*. *ERF1*: *Ethylene response factor 1*. B, defense gene that was down-regulated by HaCPL2. *COI1*: *Coronatine-insensitive 1*. Asterisks above the bars represented the statistical analysis of two-tailed unpaired t-test (* $P<0.05$, ** $P<0.01$, *** $P<0.001$, **** $P<0.0001$).

Fig. 5. Effects of HaCPL2 on Scots pine seedlings. A, overview of the seedlings 48 h after the treatments. In the control, H, V and B represented seedlings from treatment of H_2O, vector (purification products from X-33/pPICZαA culture medium) and BSA, respectively. B, Scots pine seedling roots of different treatments under stereomicroscope (scale bar: 1 mm). C, growth rate of roots 48 h after the treatments. Lower case letters above the bars represented the statistical analysis assessed with one-way analysis of variance (ANOVA) followed by Tukey's multiple comparisons at 0.05 confidence level (±SEM, n=9).

Fig. 6. Defense gene expression induced by HaCPL2 in Scots pine seedlings by RT-qPCR. Results were presented as fold change in amount of transcript levels compared to the control (±SEM, n=3). *JAZ1*: *Jasmonate zim domain protein 1*, *OPR*: *12-OPDA reductase*, *ACS*: *1-aminocyclopropane-1-carboxylic acid synthase*, *ERF1*: *Ethylene response factor 1*, *TPS*: *Terpene synthase*, *PME*: *Pectin methylesterase*, *LAC*: *Laccase*. *PAL1*: *Phenylalanine ammonia lyase 1*, *NPR1*: *Natriuretic peptide receptor 1*, and *LURP1: Late up-regulation in response to Hpa 1*. Lower case letters above the bars represented the statistical analysis assessed with one-way analysis of variance (ANOVA) within the same gene and followed by Tukey's multiple comparisons at 0.05 confidence level.

Fig. 7. Homology model of HaCPL2. A, ribbon cartoon of the model showing the conserved disulphide bond-forming cysteine residues in spring-green and relatively conserved and possible carbohydrate binding residues in gold. B, surface of the module showing hydrophilic and hydrophobic areas in light blue and orange, respectively.

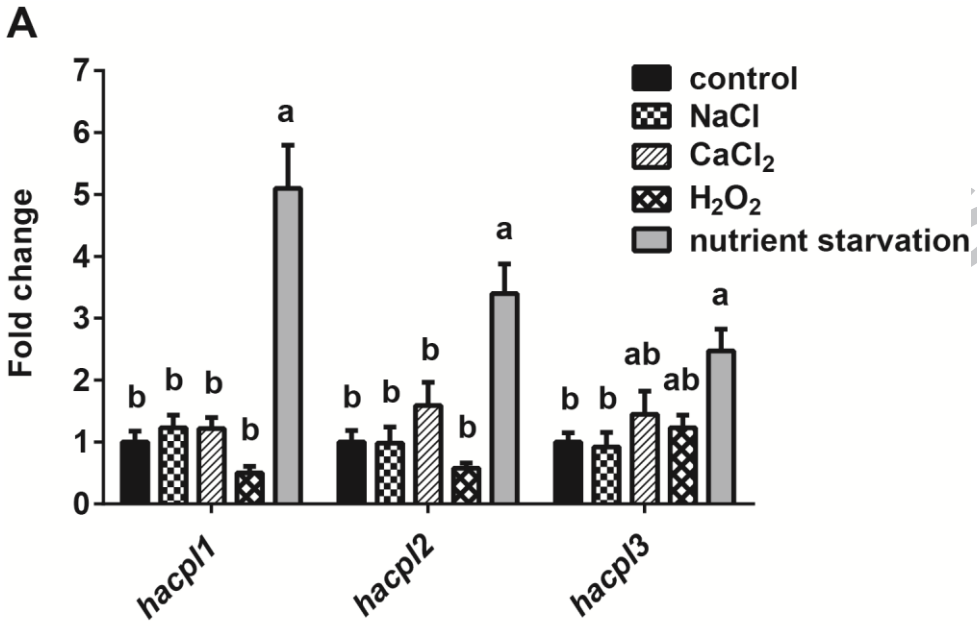

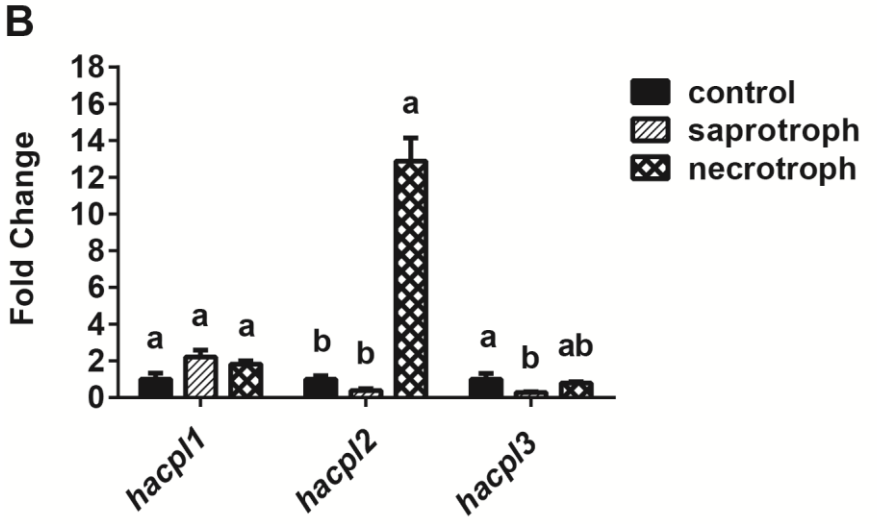

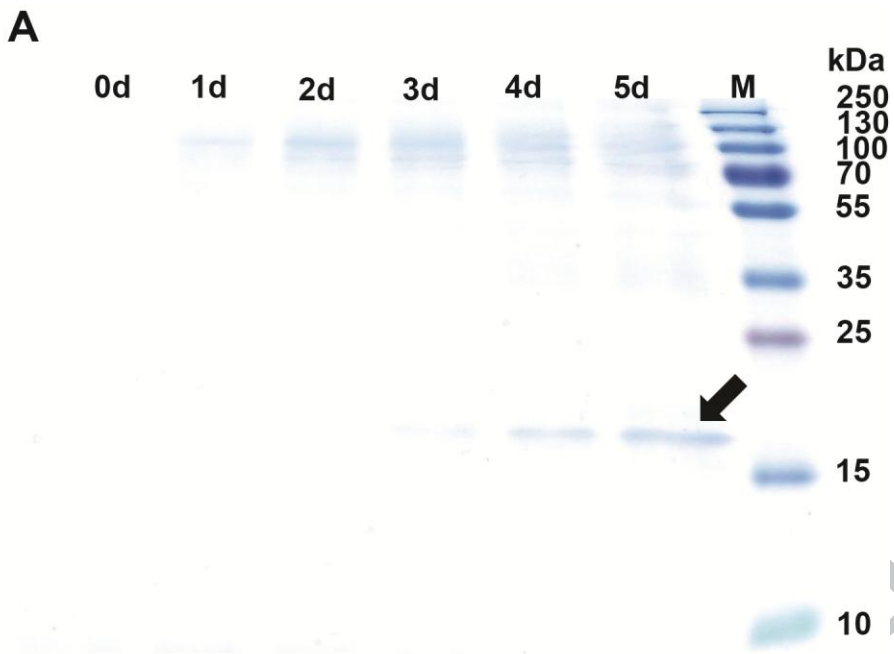

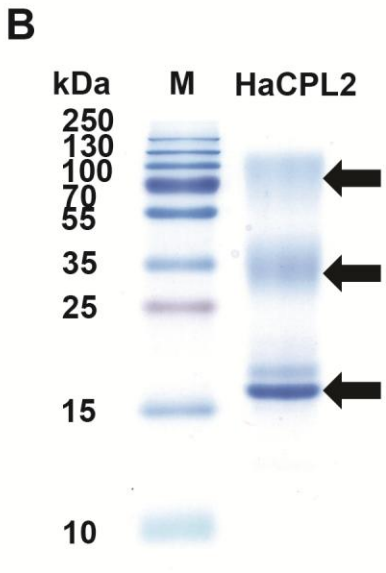

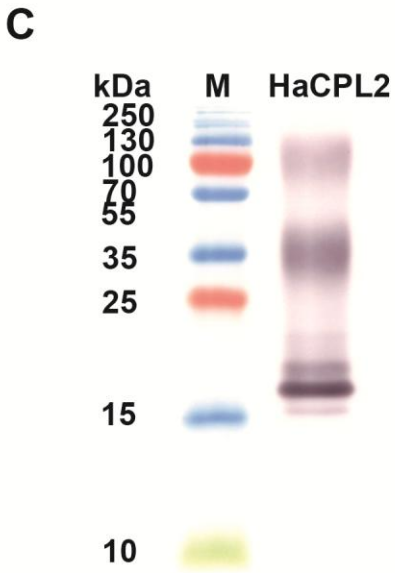

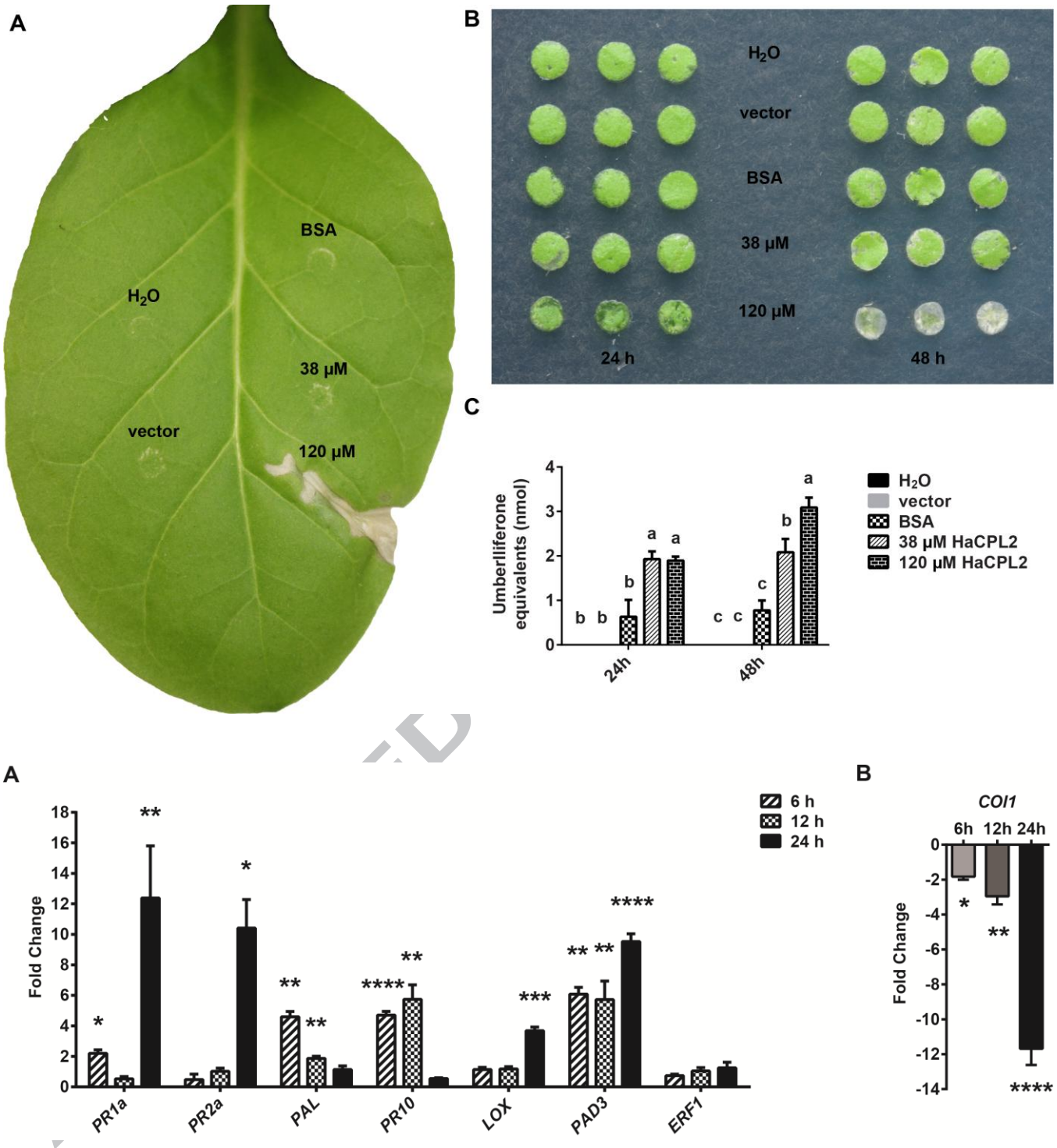

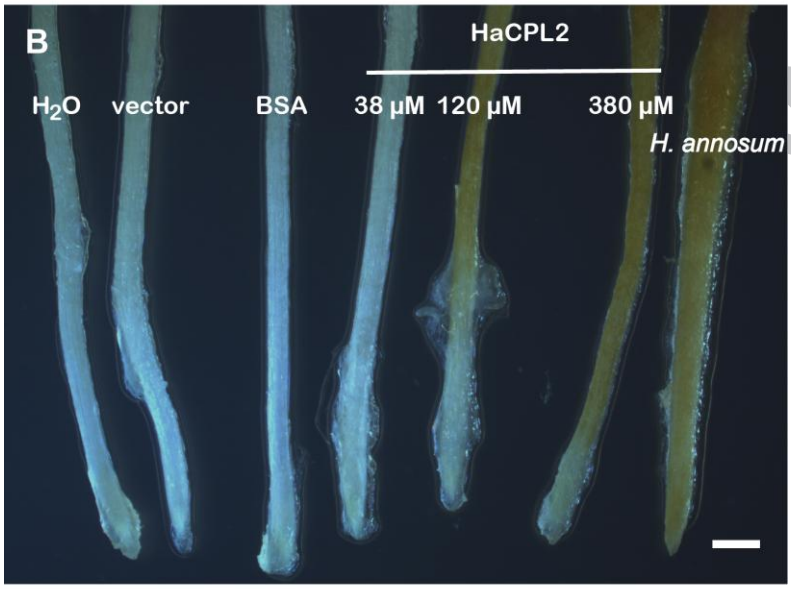

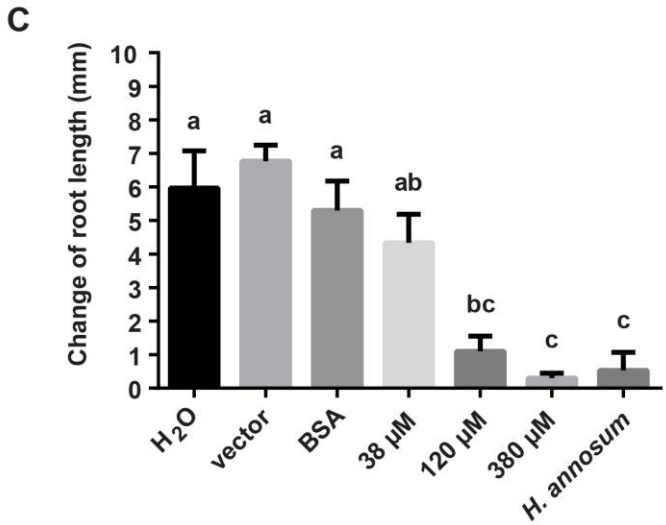

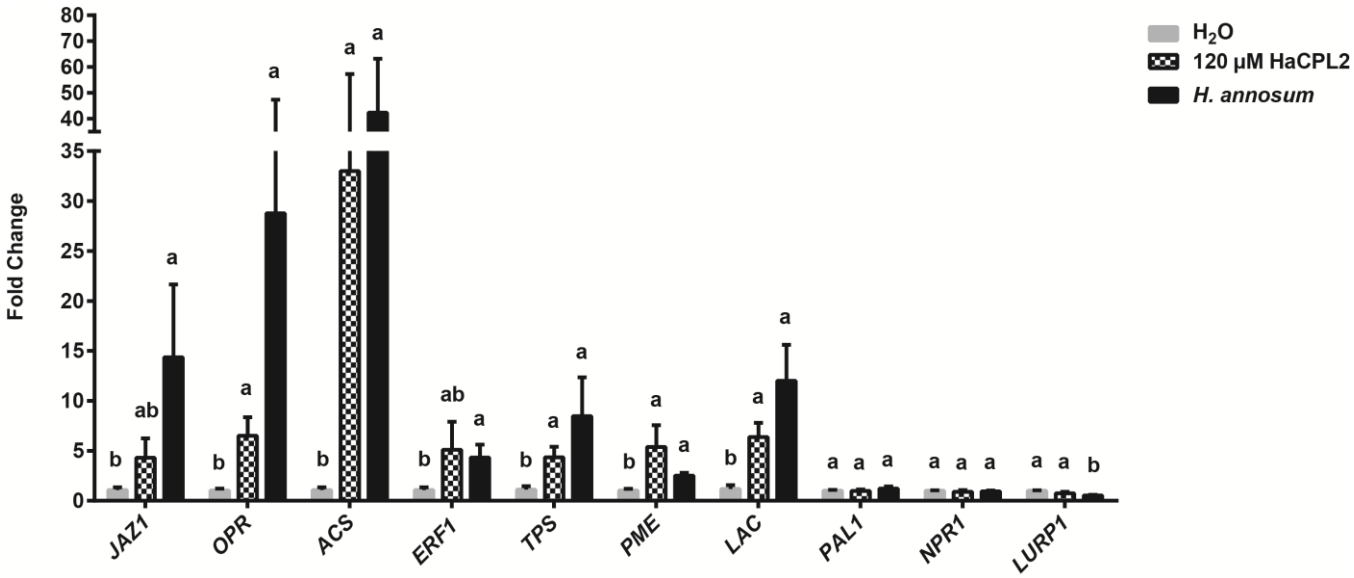

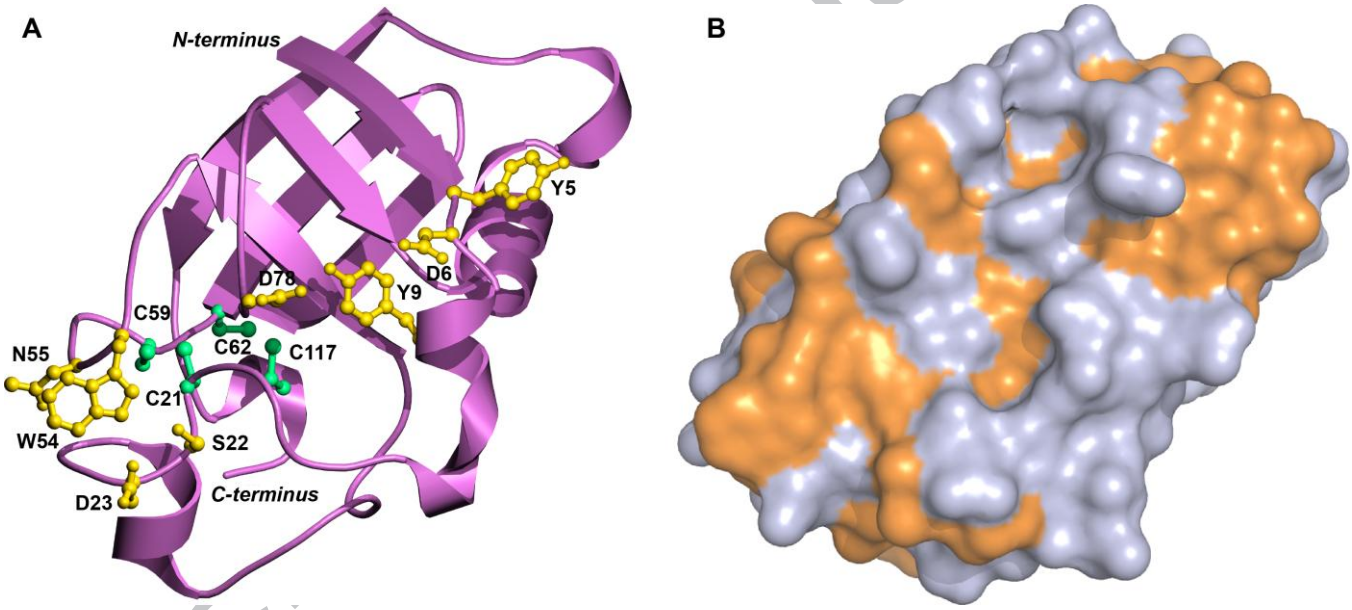

Highlights

- We characterized HaCPL2 as a cell death-inducing protein.
- *hacpl2* expression was induced during nutrient starvation and necrotrophic growth.
- HaCPL2 induced hypersensitive cell death and defense response in *N. tabacum*.
- HaCPL2 induced necrosis and inhibited the root growth on *P. sylvestris*.
- Genes related to JA and ET signaling were preferently induced in *P. sylvestris*.